IOP Publishing | Royal Swedish Academy of Sciences Physica Scripta

Phys. Scr. **89** (2014) 105203 (18pp) doi:10.1088/0031-8949/89/10/105203

Chaos control applied to cardiac rhythms represented by ECG signals

Bianca Borem Ferreira[1], **Marcelo Amorim Savi**[2] **and Aline Souza de Paula**[3]

[1] Universidade Paulista, Institute of Exact Sciences and Technology, 17.048.290, Bauru, SP, Brazil
[2] Universidade Federal do Rio de Janeiro, COPPE – Department of Mechanical Engineering, PO Box 68.503, 21.941.972, Rio de Janeiro, RJ, Brazil
[3] Universidade de Brasília, Department of Mechanical Engineering, 70.910.900, Brasília, DF, Brazil

E-mail: biaborem@gmail.com, savi@mecanica.ufrj.br and alinedepaula@unb.br

Received 23 September 2013, revised 25 June 2014
Accepted for publication 21 July 2014
Published 28 August 2014

Abstract

The control of irregular or chaotic heartbeats is a key issue in cardiology. In this regard, chaos control techniques represent a good alternative since they suggest treatments different from those traditionally used. This paper deals with the application of the extended time-delayed feedback control method to stabilize pathological chaotic heart rhythms. Electrocardiogram (ECG) signals are employed to represent the cardiovascular behavior. A mathematical model is employed to generate ECG signals using three modified Van der Pol oscillators connected with time delay couplings. This model provides results that qualitatively capture the general behavior of the heart. Controlled ECG signals show the ability of the strategy either to control or to suppress the chaotic heart dynamics generating less-critical behaviors.

Keywords: biomechanics, cardiac system, chaos control, delayed feedback control

(Some figures may appear in colour only in the online journal)

1. Introduction

The human body consists of several interconnected systems and many of them exhibit nonlinear characteristics and chaotic behavior. The heart plays a fundamental aspect in the physiology of living beings and the existence of chaotic behavior of cardiac rhythms are the objective of several research efforts (Christini *et al* 2001, Ferreira *et al* 2011, Garfinkel *et al* 1992, 1995, Glass *et al* 1983, 1987, Gois and Savi 2009, Kaplan and Cohen 1990, Savi 2005).

The heart is a hollow, muscular organ activated by electrical stimuli that promotes the pumping of blood to lungs, organs and tissues. The cardiac conduction system can be treated as a network of self-excitatory elements composed of the sino-atrial node (SA), atrio-ventricular node (AV) and the His-Purkinje system (HP) (Gois and Savi 2009, Grudzinski and Zebrowski 2004). The electric excitation is primarily generated at the SA node, known as the natural pacemaker, located at the right atrium. It initiates the electrical impulse that spreads as a wave, stimulating both atria. The impulse reaches the AV node, which is the electrical connection between the atria and the ventricles. Afterwards, the electrical impulse goes to the HP system, which transmits the electrical impulse to myocardial cells, producing simultaneous contraction of the ventricles.

The electrocardiogram (ECG) is the most widely used mechanism to analyze the heart functioning. The ECG signal records the electrical impulses related to heart function in the form of waves. Figure 1 shows the schematic sketch of an ECG signal that represents a cardiac cycle, basically composed of different waves: P, QRS complex and T. The P wave represents the electrical impulse generated by the natural pacemaker, the SA node (Santos *et al* 2004).

The dynamics of the heartbeat has been analyzed through both mathematical models and time series analysis. Van der Pol and Van der Mark (1928) carried out the first study for the dynamic description of the heart using nonlinear oscillators. Grudzinski and Zebrowski (2004) proposed a variation of the original Van der Pol oscillator in order to describe the potential action generated by a natural cardiac pacemaker. Santos *et al* (2004) presented a simplified model of cardiac dynamics composed of two asymmetrically coupled Van der Pol oscillators, representing the behavior of two cardiac pacemakers. Gois and Savi (2009) reproduced ECGs through

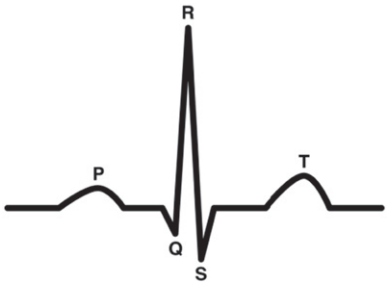

Figure 1. Schematic sketch of an ECG cardiac cycle.

a mathematical model consisting of three modified Van der Pol oscillators, which represent the SA node, AV node and the HP system, connected by time-delayed couplings. This model is able to reproduce normal and pathological ECGs.

Several studies are pointing to the fact that certain cardiac arrhythmias are instances of chaos (Witkowski *et al* 1995, 1998). Stein *et al* (1999) developed a nonlinear prediction algorithm by analyzing records of R-R intervals of sixteen patients during chronic atrial fibrillation, investigating the predictability and sensitivity to initial conditions of these datasets. The goal was to verify that the ventricular response in atrial fibrillation is chaotic, which was confirmed. In general, ventricular fibrillation is also associated with chaos.

In this regard, the control of chaotic heartbeats is a key issue of special interest in cardiology. Chaos control is based on the richness of chaotic behavior and the most important characteristic is the stabilization of unstable periodic orbits (UPO) embedded in a chaotic attractor by employing small perturbations (Shinbrot *et al* 1993, Kapitaniak 1995, Pyragas 2006). The ability to stabilize several UPOs confers to the system great flexibility that can be exploited in a variety of applications. De Paula and Savi (2011) presented a comparative analysis of the main chaos control techniques.

Chaos control has been applied to several dynamical systems, considering different purposes. Pyragas (2006) discussed several numerical and experimental applications. Andrievskii and Fradkov (2004) and Fradkov *et al* (2006) mentioned the application of control procedures to numerous systems of different fields. Mechanical systems are treated in De Paula and Savi (2008, 2009a, 2009b) who investigated a nonlinear pendulum as a representative example. De Paula *et al* (2012) investigated an electro-mechanical system employed for energy harvesting from sea waves. Chaos control and bifurcation control are successfully treated. Boccaletti *et al* (2000) treated tracking and synchronization of chaotic systems and mentioned several experimental implementations. Secure communication is also employing a chaos control approach as presented in Muthukumar *et al* (2014) and Muthukumar and Balasubramaniam (2013).

Garfinkel *et al* (1992, 1995) presented a pioneer work related to the application of a chaos control method in cardiac rhythms. They employed a perturbation feedback chaos control strategy, based on OGY approach, to stabilize cardiac arrhythmias induced by a drug called ouabain in rabbit ventricles. Hall *et al* (1997) applied the extended time delayed feedback control strategy (ETDF) in samples of the hearts of five dissected rabbits electrically stimulated in order to suppress a type of arrhythmia, known as cardiac alternans. The authors proposed a map as a model of the cardiac rhythm. Dubljevic *et al* (2008) analyzed the ability of feedback chaos control method perturbation to suppress cardiac alternans in the hearts of rabbits in real time.

Christini *et al* (2001) applied an adaptive chaos control algorithm to control a type of low-dimensional cardiac dynamics, the re-entrant arrhythmia. This technique was effective in 52 of 54 control attempts made in five patients. Attarsharghi *et al* (2009) applied an adaptive control method with delayed feedback to prevent or control pathological undesirable arrhythmias described with the aid of the logistic map to model the interval between heartbeats. López *et al* (2010) used a control algorithm with proportional gain and in the L_∞ norm of tracking error signal, applied to a cardiac model proposed by Gois and Savi (2009), in order to avoid pathological behaviors. Ferreira *et al* (2011) employed the ETDF chaos control method to the natural pacemaker modeled by the modified Van der Pol equation proposed by Grudzinski and Zebrowski (2004). The main objective was to control or to suppress chaotic responses, avoiding critical pathologies.

In this paper, the ETDF chaos control method is employed to eliminate chaotic cardiac responses. The three-coupled oscillator model proposed by Gois and Savi (2009) is employed to describe the heartbeat dynamics. The idea is to monitor ECG signals generated by the proposed model, treating two distinct situations: normal and chaotic signals. Two different approaches are presented: coupled and uncoupled. The uncoupled approach considers just the natural pacemaker to define the control perturbation evaluating its influence on the ECG signal. On the other hand, the coupled approach considers the entire system to define the perturbation control. Results show that both approaches are able to generate less complex behaviors of the ECG. It is important to highlight that the cardiac model used in this work is able to capture the general behavior of normal and pathological ECGs while most of the literature related to cardiac dynamics control considers simpler models. Thus, the novel investigation performed in this paper increases the belief that chaos control methods are able to avoid critical behavior of the heart.

This article is organized as follows. After this introduction, a brief discussion of the ETDF control method is presented including the calculation of UPO Lyapunov exponent employed to define controller parameters. The mathematical model of the cardiac system is then presented, showing normal and chaotic behaviors. Afterwards, the ETDF is applied to the cardiac system, analyzing its performance. Finally, concluding remarks are discussed.

2. Extended time-delayed feedback control method

The chaos control methods can be classified as continuous and discrete approaches. Among the continuous control

methods, the ones that stand out are the time-delayed feedback (TDF) (Pyragas 1992) and extended time-delayed feedback (ETDF) (Socolar *et al* 1994, Pyragas 1995). Among the discrete methods, it is important to highlight the pioneer OGY method (Ott *et al* 1990), the semi-continuous methods (Hubinger *et al* 1994, Korte *et al* 1995). A generalization of the discrete method is the multiparameter chaos control method (De Paula and Savi 2008, 2009b). De Paula *et al* (2012) presented a comparative analysis of chaos control methods.

The chaos control technique may be understood as a two-stage procedure. The learning stage is the first one where UPOs embedded in the system attractor are identified and controller parameters are estimated. The second stage is the control stage and consists in the use of control law to impose the perturbation needed to stabilize the desired UPO.

ETDF is a control strategy applied to systems modeled as follows (Pyragas 1992, Socolar *et al* 1994):

$$\begin{aligned} \dot{x} &= Q(x, y) \\ \dot{y} &= P(x, y) + C(t, y) \end{aligned} \tag{1}$$

where x and y are state variables, $Q(x, y)$ and $P(x, y)$ defines the system dynamics, while $C(t, y)$ is associated with the control action. In the ETDF method, the control perturbation is based on feedback from the difference between the present state and the delayed states of the system, being given by:

$$\begin{aligned} C(t, y) &= K\left[(1 - R)S_\tau - y\right] \\ S_\tau &= \sum_{m=1}^{N_\tau} R^{m-1} y_{m\tau} \end{aligned} \tag{2}$$

where $y = y(t)$, $y_{m\tau} = y(t - m\tau)$, τ is the time delay, $0 \leqslant R < 1$ and K are the controller parameters. In general, N_τ is infinite, but can be set as a function of the dynamical system. Note that, for any value of K and R, the perturbation of equation (2) is zero when the trajectory of the system is on a UPO since $y(t - m\tau) = y(t)$ for all m if $\tau = T_i$, where T_i is the periodicity of the ith UPO. According to the correct choice of the values K and R, it becomes possible to stabilize the system in one of its UPOs. The TDF is a particular case of the ETDF when $R = 0$.

Note that the dynamical system together with the control law is governed by differential difference equations (DDE). The solution of this type of equation can be carried out by considering an initial function $y_0 = y_0(t)$ over the interval $\left[-N_\tau\tau, 0\right]$. In this work, this function is estimated by a Taylor series expansion as proposed by Cunningham (1954) and shown below:

$$y_{m\tau} = y - m\tau\dot{y} \tag{3}$$

Numerical procedure considers the fourth-order Runge–Kutta method with linear interpolation on the delayed variables (Mensour and Longtin 1997). Besides, it is assumed there are three delayed states, $N_\tau = 3$.

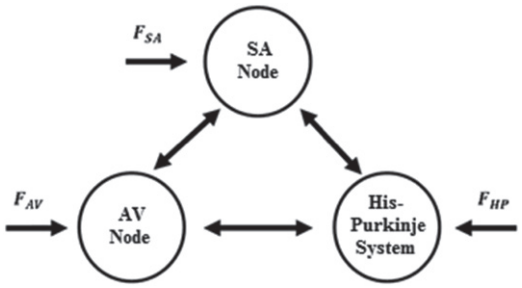

Figure 2. General conceptual model for the cardiac system.

During the learning stage, the UPO identification is carried out using the close-return method (Auerbach *et al* 1987). Moreover, controller parameters, K and R, are estimated from Lyapunov exponents of each desired UPO (De Paula and Savi 2009a, De Paula *et al* 2012, Ferreira *et al* 2011). These exponents evaluate the local divergence of nearby orbits and the idea is to look for parameters that turn the maximum exponent of the UPO negative. Their calculation is carried out by considering a finite number of elements (Farmer 1982) and therefore, the initial function, $y_i(t)$, is approximated by N samples. Under this assumption, the system is represented by $n(N + 1)$ ODEs, instead of DDEs with n state variables, and the classical algorithm proposed by Wolf *et al* (1985) is employed. For more details, see De Paula and Savi (2009a) and Ferreira *et al* (2011).

3. Mathematical model

Several studies have been developed to model the dynamics of cardiac rhythms. Basically, connected nonlinear oscillators may model the heart functioning. Each oscillator represents the cardiac systems associated with: SA node, the natural pacemaker; AV node; and HP system. The combination of waves coming from these systems is responsible for the ECG aspect.

In this work, the three-coupled oscillators model is employed to represent the ECG signal following the same idea of Gois and Savi (2009). The conceptual model of the cardiac system is presented in figure 2 where general couplings and external forcing are incorporated in order to represent different kinds of behavior.

A modified Van der Pol equation proposed by Grudzinski and Zebrowski (2004) is employed to mathematically represent the cardiac system. Therefore, the system is governed by the following equations.

$$\begin{aligned} \dot{x}_1 &= x_2 \\ \dot{x}_2 &= F_{SA}(t) - \alpha_{SA} x_2 (x_1 - v_{SA_1})(x_1 - v_{SA_2}) \\ &\quad - \frac{x_1 (x_1 + d_{SA})(x_1 + e_{SA})}{d_{SA} e_{SA}} \\ &\quad - k_{AV-SA}\left(x_1 - x_3^{\tau_{AV-SA}}\right) - k_{HP-SA}\left(x_1 - x_5^{\tau_{HP-SA}}\right) \end{aligned}$$

$$\dot{x}_3 = x_4$$
$$\dot{x}_4 = F_{AV}(t) - \alpha_{AV} x_4 (x_3 - v_{AV_1})(x_3 - v_{AV_2}) - \frac{x_3 (x_3 + d_{AV})(x_3 + e_{AV})}{d_{AV} e_{AV}} - k_{SA-AV}\left(x_3 - x_1^{\tau_{SA-AV}}\right) - k_{HP-AV}\left(x_3 - x_5^{\tau_{HP-AV}}\right)$$
$$\dot{x}_5 = x_6$$
$$\dot{x}_6 = F_{HP}(t) - \alpha_{HP} x_6 (x_5 - v_{HP_1})(x_5 - v_{HP_2}) - \frac{x_5 (x_5 + d_{HP})(x_5 + e_{HP})}{d_{HP} e_{HP}} - k_{SA-HP}\left(x_5 - x_1^{\tau_{SA-HP}}\right) - k_{AV-HP}\left(x_5 - x_3^{\tau_{AV-HP}}\right), \quad (4)$$

where $F_{SA}(t) = \rho_{SA} \sin(\omega_{SA} t)$, $F_{AV}(t) = \rho_{AV} \sin(\omega_{AV} t)$ and $F_{HP}(t) = \rho_{HP} \sin(\omega_{HP} t)$ are harmonic external excitations applied to each oscillator; α_{SA}, α_{AV}, α_{HP}, v_{SA_1}, v_{AV_1}, v_{HP_1}, v_{SA_2}, v_{AV_2}, v_{HP_2}, d_{SA}, d_{AV}, d_{HP}, e_{SA}, e_{AV}, e_{HP} are system parameters; k_{AV-SA}, k_{HP-SA}, k_{SA-AV}, k_{HP-AV}, k_{SA-HP} and k_{AV-HP} are coupling constants; $x_i^{\tau} = x_i(t - \tau)$, with τ representing the delay; $i = 1, \ldots, n$, where n is the dimension of the system. Note that the coupling terms have time delay, x_i^{τ}, which represents the time necessary for the transmission of signals between different regions of the heart.

Gois and Savi (2009) suggested that the ECG signal is formed by the composition of individual signals of the oscillators, and its representation can be done by a linear combination of each oscillator signal as follows:

$$X = ECG = \beta_0 + \beta_1 x_1 + \beta_2 x_3 + \beta_3 x_5 \quad (5)$$

Similarly, it is defined:

$$\dot{X} = \frac{d(ECG)}{dt} = \beta_1 x_2 + \beta_2 x_4 + \beta_3 x_6 \quad (6)$$

3.1. ECG signals

This section deals with numerical simulations of the proposed model showing its capacity to describe some typical ECG signals. Our main goal is to show a qualitative agreement with experimental ECG signals, especially the normal and some pathological signals related to chaotic behavior.

In all simulations time steps are defined as $\Delta t = 2\pi / N_M \omega$, with $N_M \geqslant 150$, $N_P = 30\,000$ and $\omega = \omega_{AV}$. Moreover, the following initial conditions are adopted:

$$\left[x_1(0) \;\; x_2(0) \;\; x_3(0) \;\; x_4(0) \;\; x_5(0) \;\; x_6(0)\right] = [-0.1 \; 0.025 \; -0.6 \; 0.1 \; -3.3 \; 10/15].$$

3.1.1. Normal ECG. The normal ECG is now in focus by considering the following parameters: $\alpha_{SA} = 3$, $v_{SA1} = 1$, $v_{SA2} = -1.9$, $d_{SA} = 1.9$, $e_{SA} = 0.55$, $\alpha_{AV} = 3$, $v_{AV1} = 0.5$, $v_{AV2} = -0.5$, $d_{AV} = 4$, $e_{AV} = 0.67$, $\alpha_{HP} = 7$, $v_{HP1} = 1.65$, $v_{HP2} = -2$, $d_{HP} = 7$, $e_{HP} = 0.67$, $\beta_0 = 1\,mV$, $\beta_1 = 0.06\,mV$, $\beta_2 = 0.1\,mV$, $\beta_3 = 0.3\,mV$, $k_{SA-AV} = 3$, $k_{AV-HP} = 55$, $\tau_{SA-AV} = 0.8$, $\tau_{AV-HP} = 0.1$. Note that this is related to a conceptual model with unidirectional couplings as presented in figure 3.

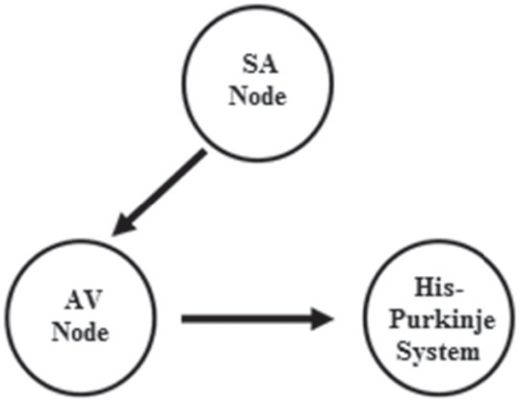

Figure 3. Conceptual model of the normal ECG.

Figure 4 shows the comparison between numerical simulations and an experimental normal ECG obtained from the Physionet database[4]. It is noticeable that the numerical ECG captures the general behavior of a normal ECG, showing good agreement with real data. Furthermore, analyzing the detail of a cardiac cycle it is observed that the numerical ECG presents the three basic waves: P wave, QRS complex and T wave. It is also important to observe the periodic, regular behavior of this kind of response.

Another way to observe ECG behavior is from phase space and Poincaré sections. Figure 5 presents two-dimensional projections of phase space while figure 6 presents Poincaré sections that show a stroboscopic view of the system dynamics. Results show a regular behavior. Phase space projections have regular behavior characterized by closed curves. On the other hand, the observation of Poincaré sections point to a quasi-periodic response due to the closed curve aspect of the response.

The regular characteristic of the normal ECG can be assured by the estimation of Lyapunov exponents that is done by conslidering the algorithm due to Wolf *et al* (1985) using the procedure discussed in De Paula and Savi (2009a). Under this assumption, it furnishes the following final values: $\lambda = (0 \;\; 0 \;\; -0.2 \;\; -0.2 \;\; -4.5 \;\; -4.6)$. Since this spectrum does not present positive values, it is possible to conclude that the system does not present local divergence and hence, the response is not chaotic. This result confirms the quasi-periodic aspect observed in the Poincaré section.

3.1.2. Chaotic ECG. Several research studies indicate situations related to the chaotic behavior of the heart. Fibrillation is a kind of arrhythmia related to irregular behavior and, typically, there are two possibilities: atrial and ventricular fibrillations. Atrial fibrillation is a fast irregular heart rhythm that can cause blood clots, stroke and heart failure. In this pathology, several electrical impulses compete generating an irregular response of the ventricles. Ventricular

[4] www.physionet.org/physiobank/database/#ecg.

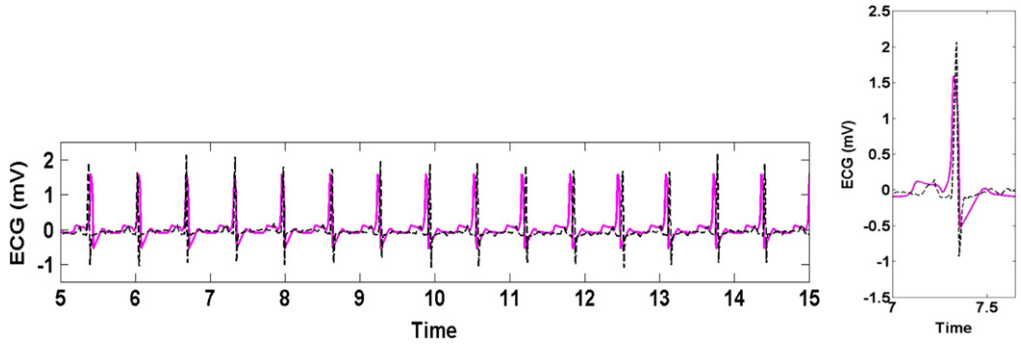

Figure 4. Comparison between numerical (dashed black line) and experimental (pink line) data of the normal ECG from Physionet.

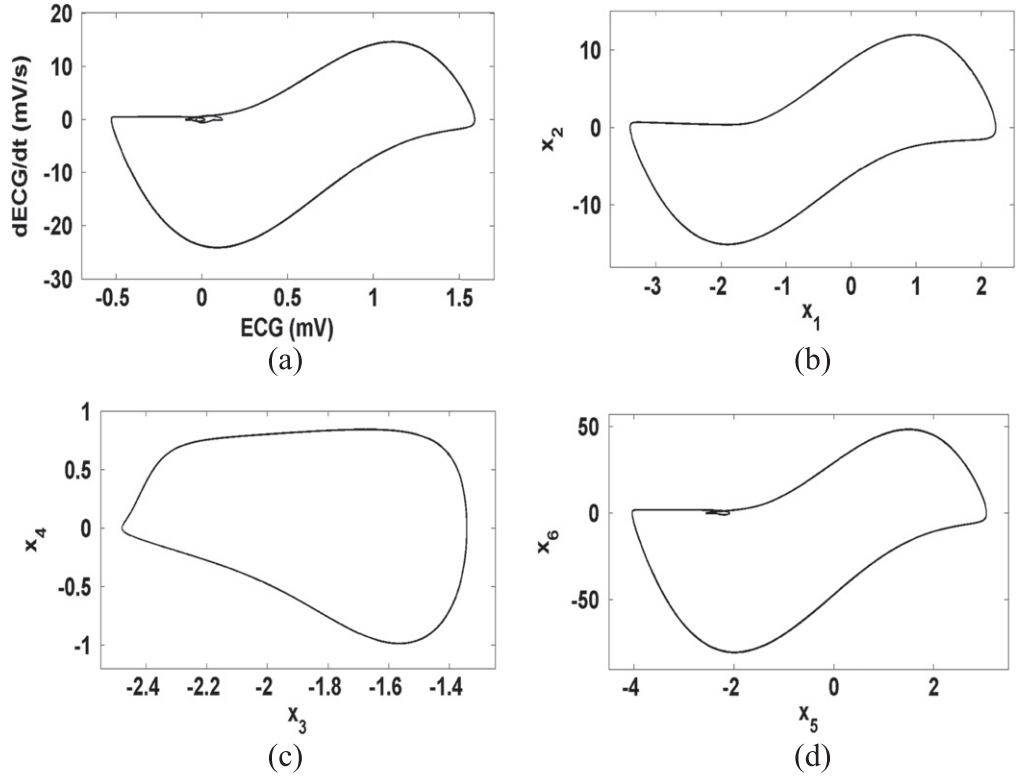

Figure 5. Phase space projections related to normal ECG: (a) ECG; (b) SA node; (c) AV node; (d) HP system.

fibrillation is a severe cardiac arrhythmia usually associated with chaotic and irregular ventricular contraction (Dubin 1996). This behavior causes a lack of synchronization necessary for the proper functioning of the heart. This pathological behavior of the heart is critical, being responsible for death.

Chaotic ECGs have an irregular aspect that can vary from different measures. Figure 7 presents different chaotic ECGs related to atrial and ventricular fibrillation. Note that there are distinct patterns associated with these behaviors. The first three ECGs (a, b, c) are related to atrial fibrillation while the last three (d, e, f) are associated with ventricular fibrillation.

Here, a chaotic ECG is considered assuming the conceptual model shown in figure 8. The model parameters are similar to the one used for the normal ECG, except for the parameters related to the SA node (Ferreira *et al* 2011): $\alpha_{SA} = 0.5$, $v_{SA1} = 0.97$, $v_{SA2} = -1$, $d_{SA} = 3$ and $e_{SA} = 6$. Besides, external excitation is considered by assuming the following parameters: $\rho_{SA} = 2.5$, $\omega_{SA} = 1.9$, $\rho_{AV} = 5$, $\omega_{AV} = 1.9$, $\rho_{HP} = 20$ and $\omega_{HP} = 1.9$.

Figure 9 shows numerical simulations related to the chaotic ECG. An irregular pattern is noticeable being characterized by a non-periodic aspect of the ECG (figure 9). Note that the ECG does not present a sequence of repeated peaks, characterizing a non-periodic response. This irregular pattern properly represents the qualitative behavior of some experimental ECGs. Another possibility for observing this kind of behavior is using phase space and Poincaré sections, presented in figures 10 and 11. Phase space projections have

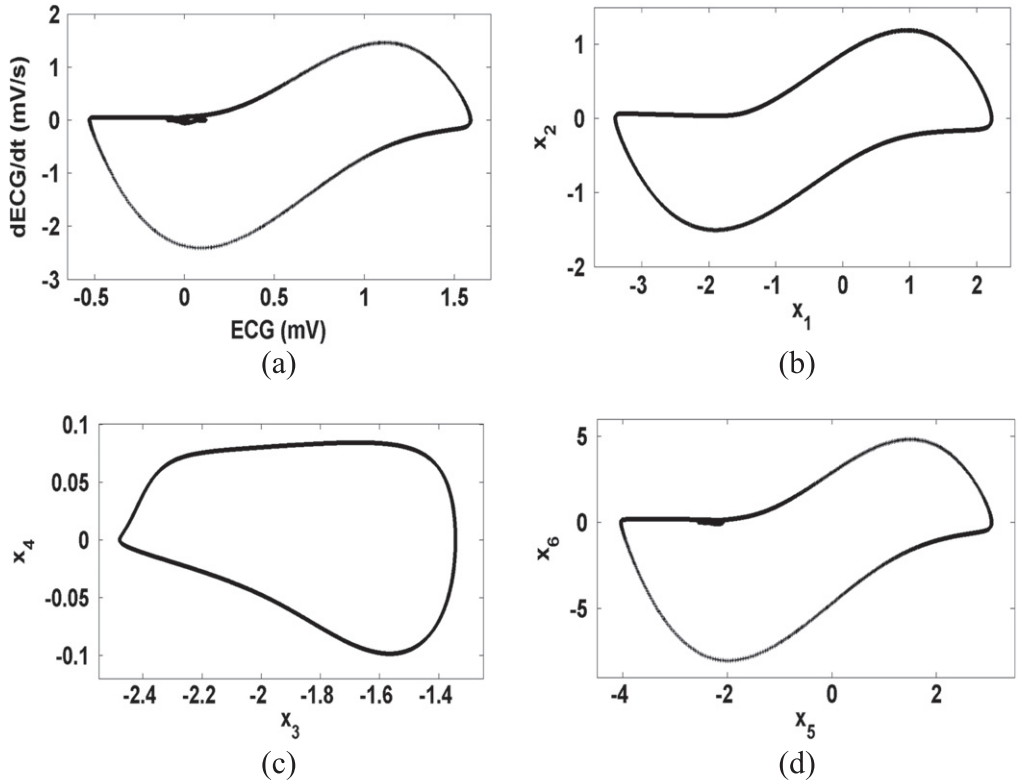

Figure 6. Poincaré section projections related to normal ECG: (a) ECG; (b) SA node; (c) AV node; (d) HP system.

an irregular aspect characterized by curves that never close. Poincaré sections, on the other hand, present a fractal-like structure. This kind of behavior is typical of chaotic responses and this conclusion can be assured by estimating Lyapunov exponents. Once again, the algorithm due to Wolf *et al* (1985) is employed using the procedure presented by De Paula and Savi (2009a) furnishing the following set: $\lambda = \left(+0.2 \;\; +0.2 \;\; -0.4 \;\; -0.4 \;\; -2.1 \;\; -2.1\right)$. Note that there are two positive values that characterize the local divergence of nearby orbits, confirming the chaotic nature of this pathology.

4. Chaos control applied to cardiac system

The ETDF approach is now applied to the heart rhythms. The goal is to control the chaotic ECG. Under this assumption, we consider system perturbations that avoid this pathology. The control action is included in the natural pacemaker, the SA node. The most interesting idea would be to stabilize a UPO related to the normal ECG. Nevertheless, the search for and the choice of this UPO is not an easy task and therefore, we choose some arbitrary UPOs in order to observe the general behavior of the controlled system, trying to avoid critical pathological behavior of the cardiac system.

The control action, represented by $C(t, x_2)$, is applied at the SA node (natural pacemaker) and the system dynamics is governed by the following equations.

$$
\begin{aligned}
\dot{x}_1 &= x_2 \\
\dot{x}_2 &= F_{SA}(t) - \alpha_{SA} x_2 (x_1 - v_{SA_1})(x_1 - v_{SA_2}) \\
&\quad - \frac{x_1 (x_1 + d_{SA})(x_1 + e_{SA})}{d_{SA} e_{SA}} - k_{AV-SA}\left(x_1 - x_3^{\tau_{AV-SA}}\right) \\
&\quad - k_{HP-SA}\left(x_1 - x_5^{\tau_{HP-SA}}\right) + C(t, x_2) \\
\dot{x}_3 &= x_4 \\
\dot{x}_4 &= F_{AV}(t) - \alpha_{AV} x_4 (x_3 - v_{AV_1})(x_3 - v_{AV_2}) \\
&\quad - \frac{x_3 (x_3 + d_{AV})(x_3 + e_{AV})}{d_{AV} e_{AV}} \\
&\quad - k_{SA-AV}\left(x_3 - x_1^{\tau_{SA-AV}}\right) - k_{HP-AV}\left(x_3 - x_5^{\tau_{HP-AV}}\right) \\
\dot{x}_5 &= x_6 \\
\dot{x}_6 &= F_{HP}(t) - \alpha_{HP} x_6 (x_5 - v_{HP_1})(x_5 - v_{HP_2}) \\
&\quad - \frac{x_5 (x_5 + d_{HP})(x_5 + e_{HP})}{d_{HP} e_{HP}} \\
&\quad - k_{SA-HP}\left(x_5 - x_1^{\tau_{SA-HP}}\right) - k_{AV-HP}\left(x_5 - x_3^{\tau_{AV-HP}}\right)
\end{aligned}
\tag{7}
$$

The controller adopted a wait time approach to start its actuation. This means that the actuation only starts when the system visits the neighborhood of the desired UPO. This is a standard procedure for discrete chaos control methods (De Paula *et al* (2012)) and presents good results in cardiac systems (Ferreira *et al* 2011).

After UPO identification, it is necessary to define controller parameters, K and R, which is done by the calculation

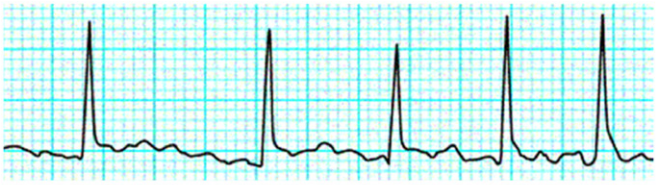

(a) (www.medicinageriatrica.com.br)

(b) (www.dzai.com.br)

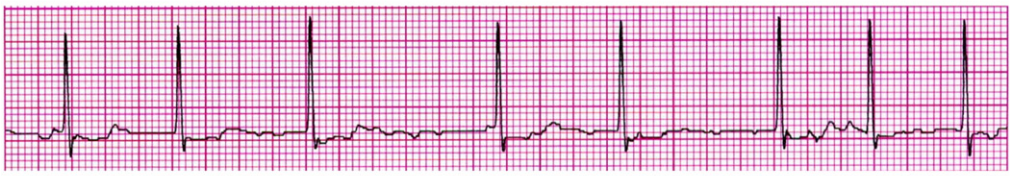

(c) (healthsciences.utah.edu)

(d) (www.geicpe-tripod-com)

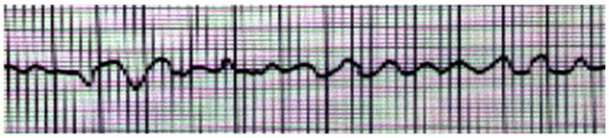

(e) (users.matrix.com.br/grace/fv.html)

(f) (www.nigeriandoctor.com)

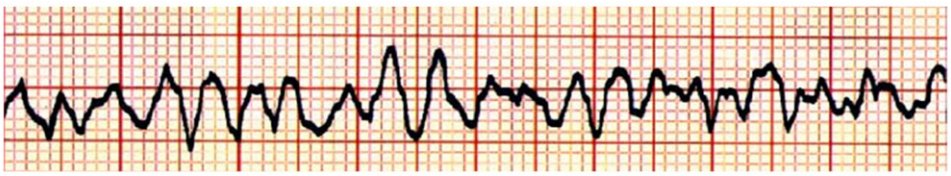

(g) (www.ecg.med.br)

Figure 7. Irregular ECGs related to atrial (a)–(c) and ventricular (d)–(g) fibrillation.

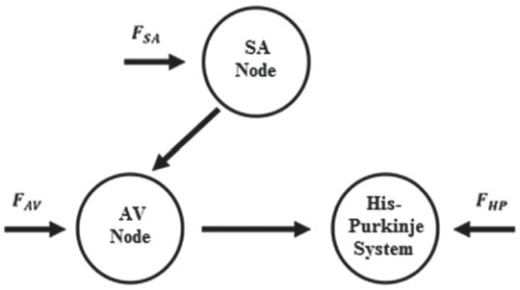

Figure 8. Conceptual model of the chaotic ECG.

of maximum Lyapunov exponents for each desired UPO. Let us start the analysis by considering a period-2 UPO. Figure 12 shows the identified orbit through the two-dimensional projections of the phase space. Figure 13 presents the maximum Lyapunov exponents, considering $\tau = 2(2\pi/\omega)$, corresponding to the periodicity 2. Note that there are regions associated with negative values of Lyapunov exponents, where it is possible to stabilize UPOs with proper choices of parameters R and K.

The controller performs the stabilization of the period-2 UPO adopting $R = 0$ and $K = 0.4$. Figure 14 shows the uncontrolled (chaotic—dashed black line) and the controlled (pink line) ECGs. Figure 15 shows the same behavior by observing phase space projections while figure 16 presents the control action imposed on the system. Note that it is possible to minimize the effects of chaotic cardiac response using small perturbations.

The stabilization of a period-4 UPO is now in focus. Figure 17 shows two-dimensional projections of the phase space orbits. Figure 18 shows the maximum Lyapunov exponents for different control parameters, considering $\tau = 4(2\pi/\omega)$, associated with the periodicity 4. Note that the stabilization of the orbit can be obtained for a range of values of K, when $R = 0$, $R = 0.2$ and $R = 0.4$. Thus, we adopt $R = 0$ and $K = 0.8$.

Figure 19 shows uncontrolled (chaotic—dashed black line) and controlled (solid pink line) responses of the heart system in the form of ECG. Phase space projections are presented in figure 20 for both situations while figure 21 presents the control action imposed on the system. Once

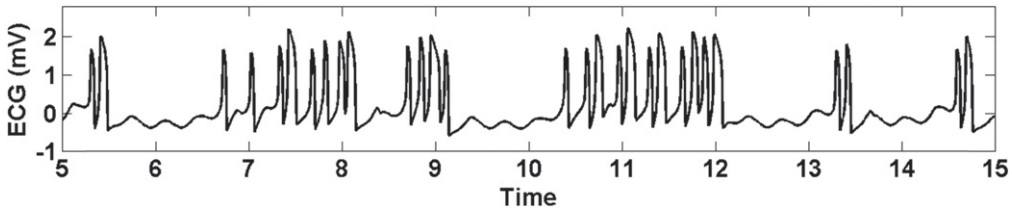

Figure 9. Numerical simulation of a chaotic ECG.

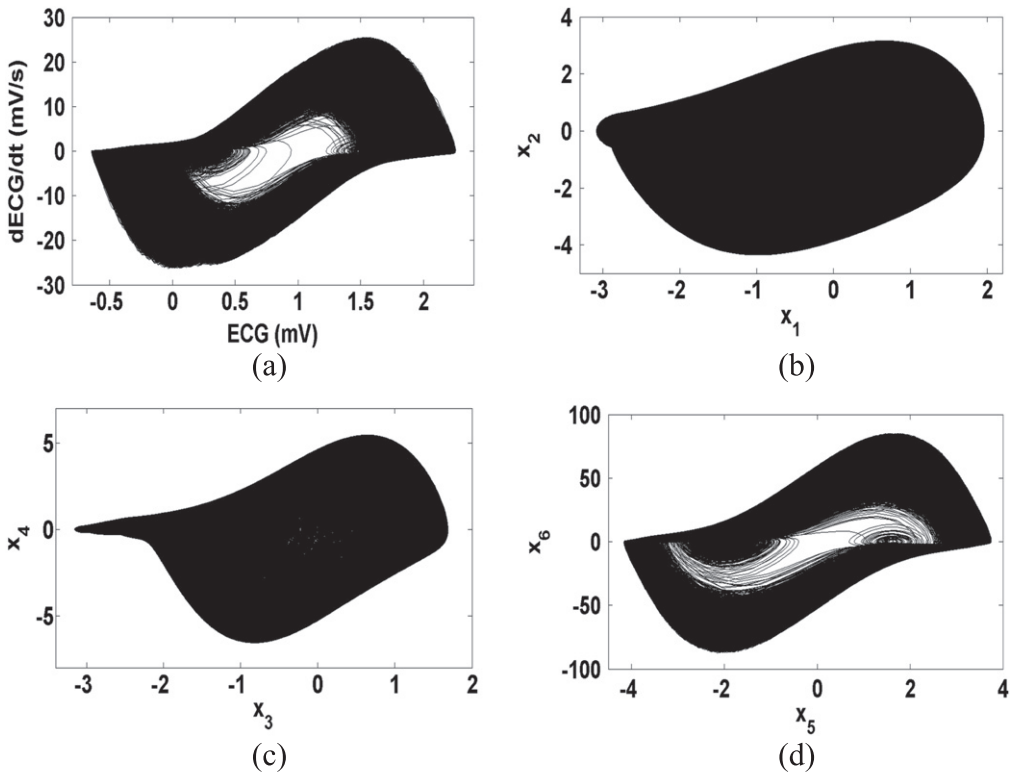

Figure 10. Phase space projections related to chaotic ECG: (a) ECG; (b) SA node; (c) AV node; (d) HP system.

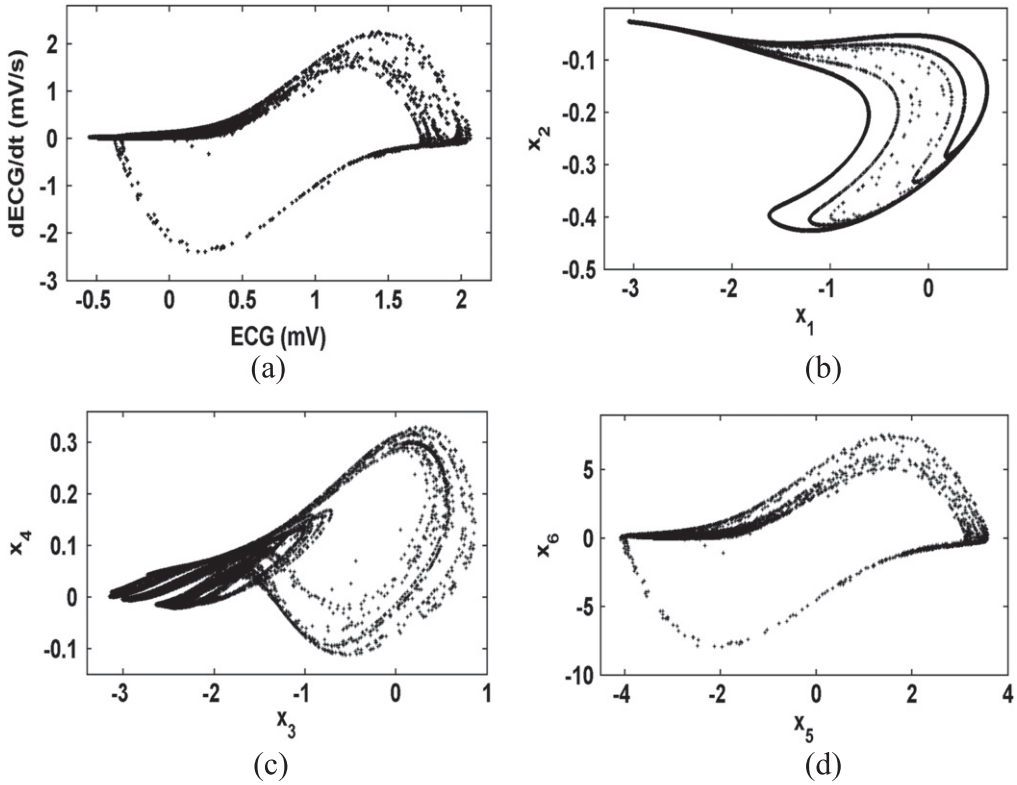

Figure 11. Poincaré section projections related to chaotic ECG: (a) ECG; (b) SA node; (c) AV node; (d) HP system.

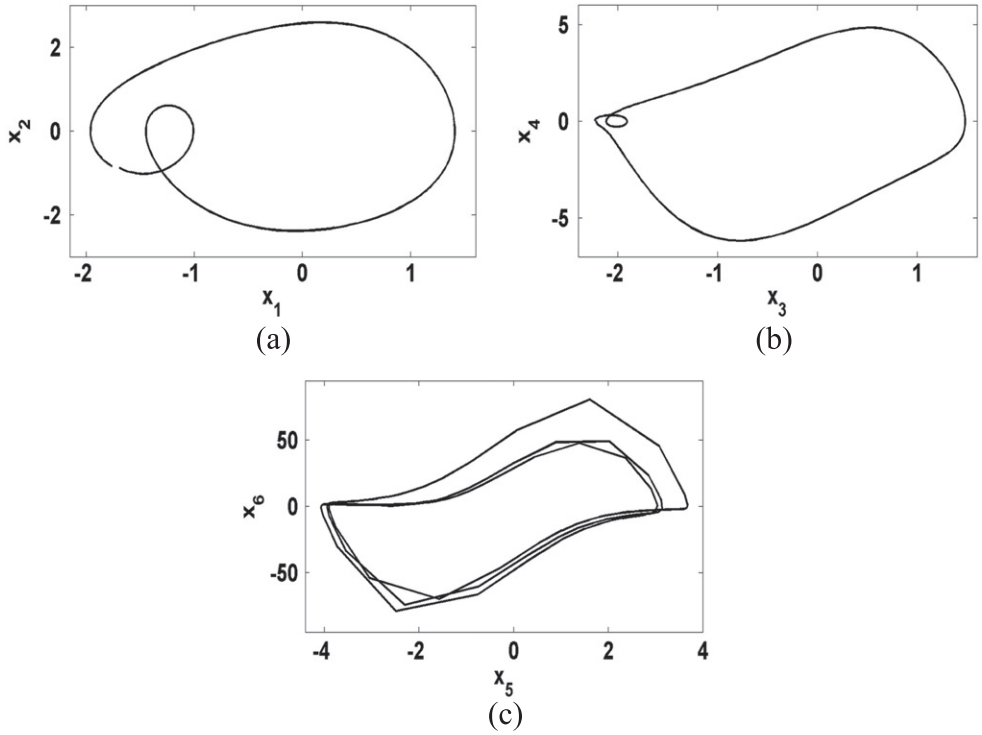

Figure 12. Identified period-2 UPO: (a) SA node, (b) AV node and (c) HP system.

again, the controller is able to stabilize the UPO, bringing the heart system to present a less critical behavior.

A different period-4 UPO is now analyzed. Figure 22 shows the identified orbit through the two-dimensional projections and figure 23 presents the maximum Lyapunov exponents considering $\tau = 4(2\pi/\omega)$. It is found that the stabilization of the orbit can be obtained for a small range of values of K, when $R = 0.4$. Hence, $R = 0.4$ and $K = 0.4$ are

adopted for control purposes. Figure 24 establishes a comparison between uncontrolled (ventricular fibrillation—dashed black line) and controlled (solid pink line) ECGs, while figures 25 and 26 present, respectively, two-dimensional projections of the phase spaces, associated with both systems, and control action. Note that the controller is able to promote this stabilization, however, greater control effort is necessary when compared to the previous period-4 UPO.

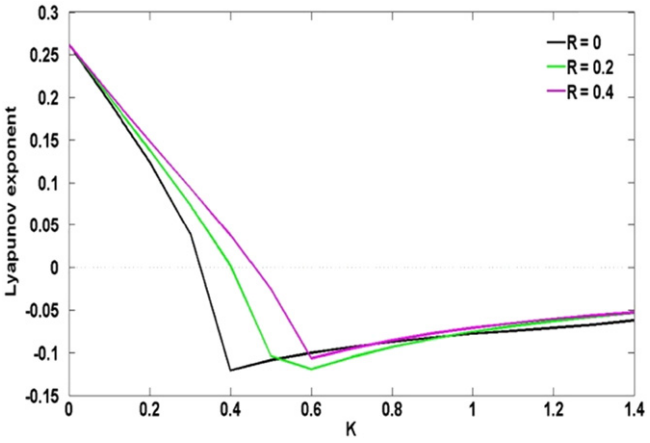

Figure 13. Period-2 UPO: maximum Lyapunov exponents.

4.1. Chaos suppression

The stabilization of a UPO embedded in a chaotic attractor is very convenient since this orbit belongs to system dynamics and therefore its stabilization requires less controller effort. Nevertheless, there are some situations where this is not possible. In these cases, chaos suppression is an interesting alternative in order to avoid critical pathological behavior of the cardiac system. The major difference between both cases is that chaos suppression is associated with larger control efforts. This procedure evades the central idea of chaos control that uses small perturbations but it is useful for health issues.

In this regard, let us consider the stabilization of a period-7 UPO presented in figure 27. Figure 28 shows the maximum

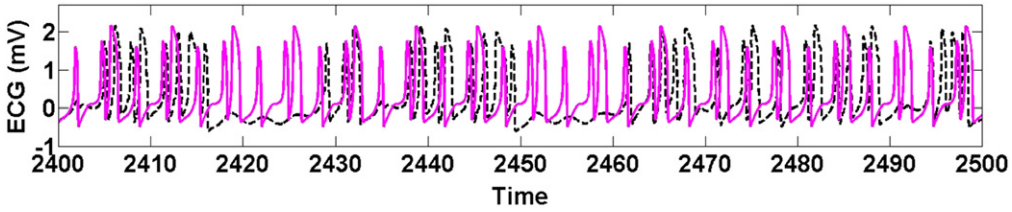

Figure 14. Chaotic ECG and the stabilization of a period-2 UPO: uncontrolled (dashed black line) and controlled (solid pink line) responses using $R = 0$ and $K = 0.4$.

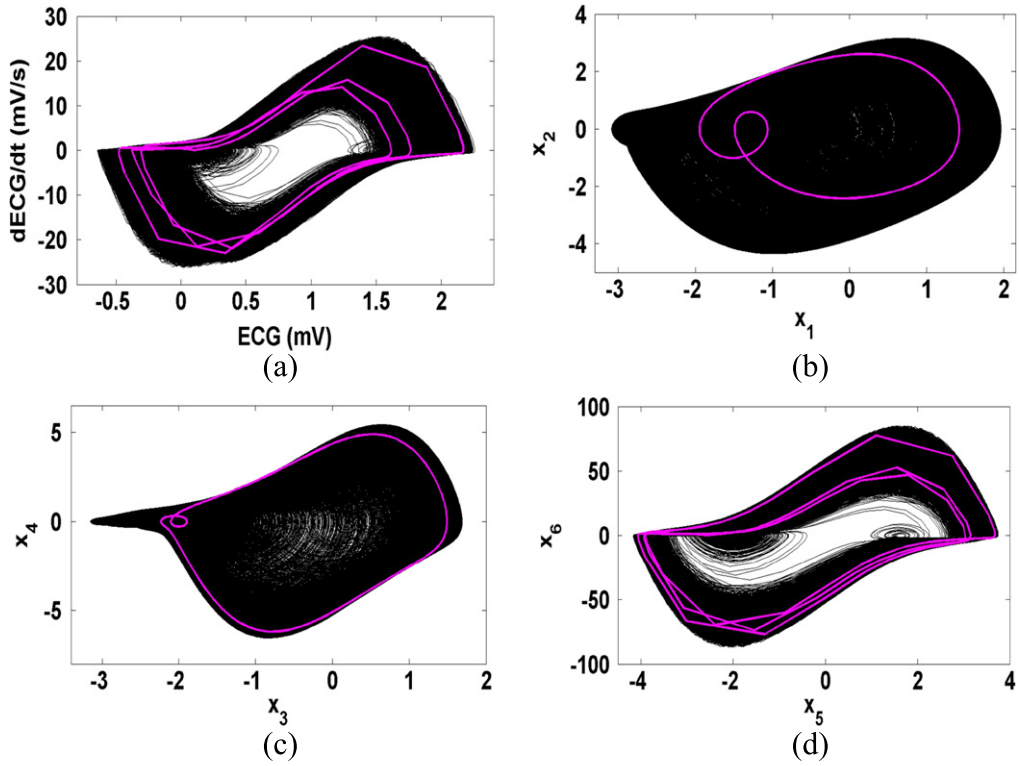

Figure 15. Phase space projection related to the chaotic ECG and the stabilization of a period-2 UPO: uncontrolled (black line) and controlled (pink line) responses using $R = 0$ and $K = 0.4$. (a) ECG, (b) SA node, (c) AV node and (d) HP system.

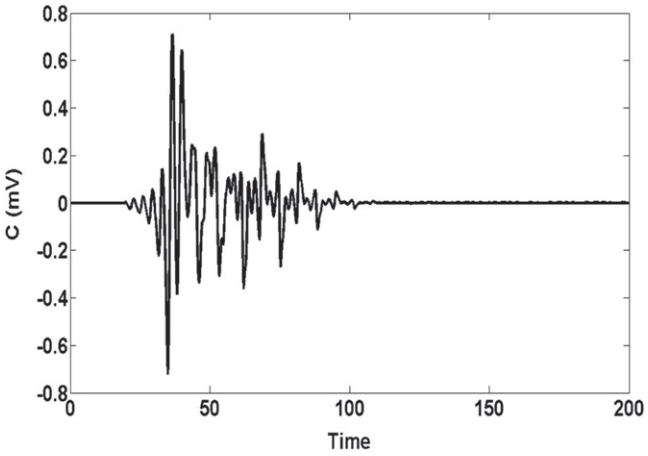

Figure 16. Control action for the stabilization of a period-2UPO.

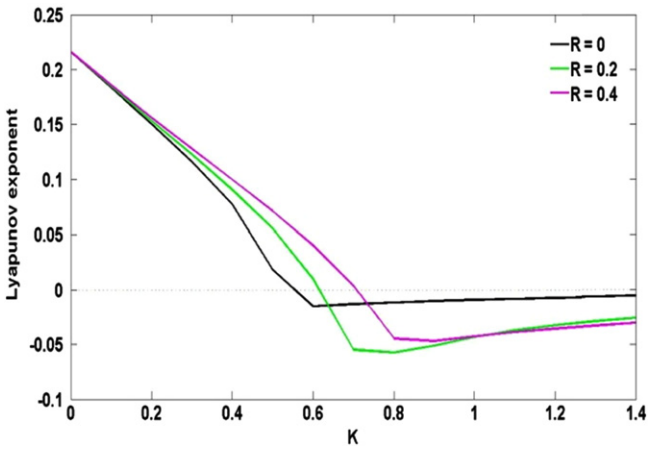

Figure 18. Period-4 UPO: maximum Lyapunov exponents.

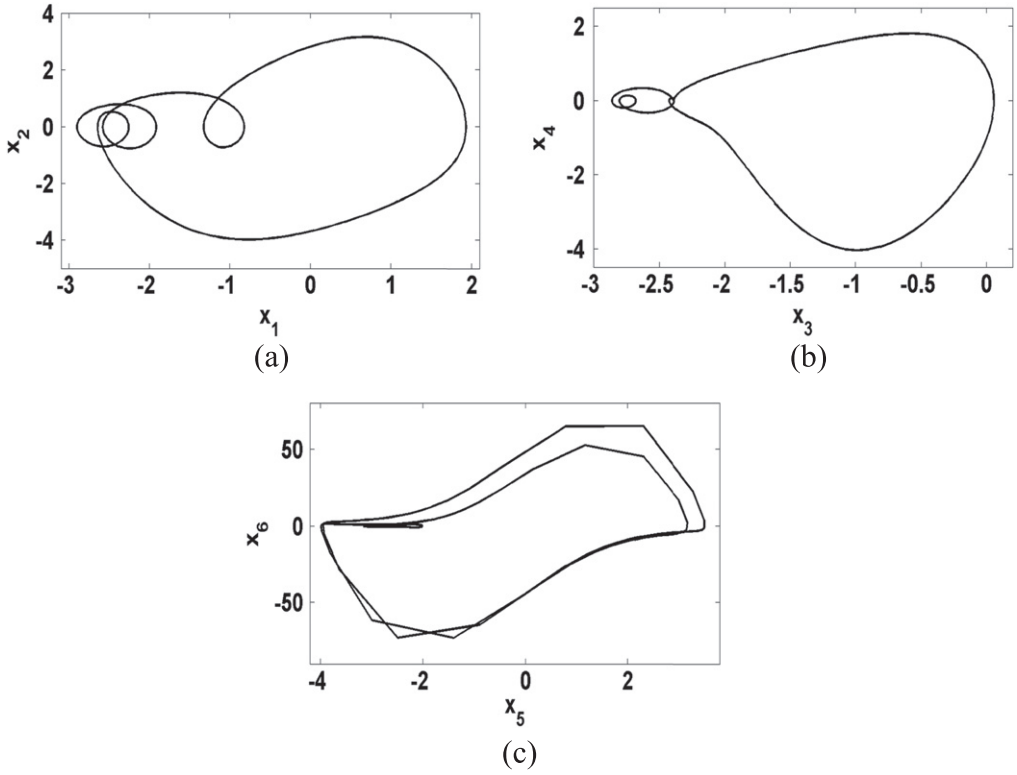

Figure 17. Identified period-4 UPO: (a) SA node, (b) AV node and (c) HP system.

Lyapunov exponents considering $\tau = 7(2\pi/\omega)$, which corresponds to periodicity 7. Note that the system does not present any negative exponent, and therefore, it is not possible to stabilize this orbit. This result can be expected due to the difficulty of the ETDF approach to target orbits with high periodicity (Pyragas 2006).

Although the stabilization of UPOs is not possible with this range of parameters, the idea of chaos control can be extrapolated employing some other controller parameters. Under this assumption, the following parameters are employed: $R = 0.8$ and $K = 2$. Figure 29 shows the ECG record of the uncontrolled (chaotic—black dashed line) and the controlled (solid pink line) responses. Figure 30 shows the phase space projections related to both responses while figure 31 presents the control action.

A different set of controller parameters are now adopted: $R = 0.9$ and $K = 0.6$. Under this assumption, a period-2 orbit is stabilized as shown in figures 32–34 that respectively present ECG, phase space projections and control action.

These results show that the controller is able to suppress the chaotic behavior of the heart. However, it should be highlighted that the stabilized orbits are not related to natural orbits of the system and, as a consequence, the controller

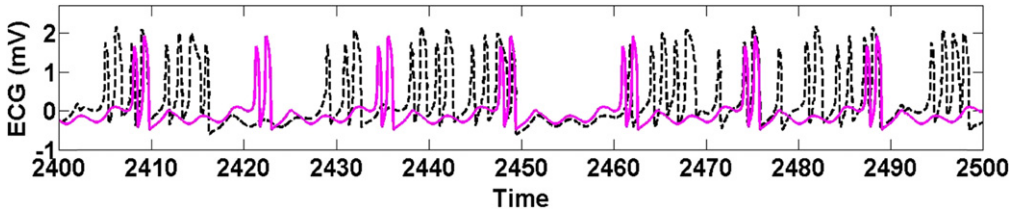

Figure 19. Chaotic ECG and the stabilization of a period-4 UPO: uncontrolled (dashed black line) and controlled (solid pink line) responses using $R = 0$ and $K = 0.8$.

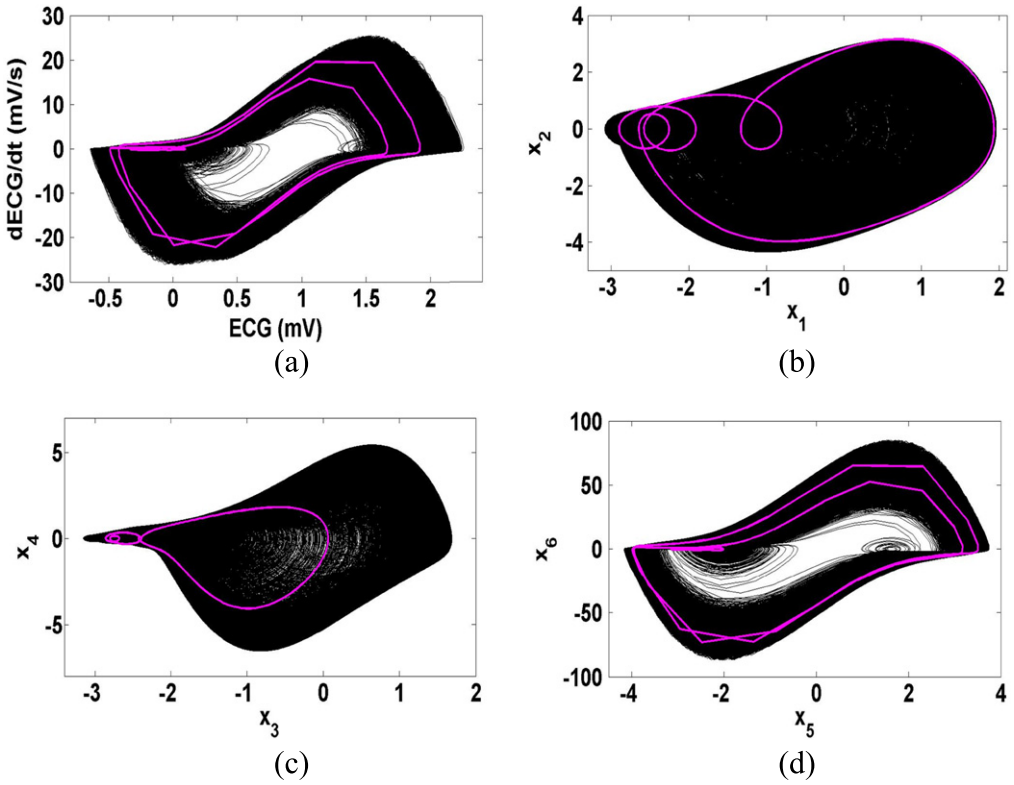

Figure 20. Phase space projections related to chaotic ECG and the stabilization of a period-4 UPO: uncontrolled (black line) and controlled (pink line) responses using $R = 0$ and $K = 0.8$. (a) ECG, (b) SA node, (c) AV node and (d) HP system.

efforts are greater than situations where orbits that belong to system dynamics are stabilized.

4.2. Uncoupled approach

Since the normal functioning of the heart system does not present all couplings discussed in the general model, it is possible to consider alternative approaches to perform chaos control. In this regard, we define the uncoupled approach in such a way that the system dynamics is analyzed by considering subsystems of the original model, composed by three-coupled oscillators (SA, AV and HP). The idea is to use two subsystems: SA node and AV-HP subsystem. All control purposes are evaluated from the SA node and therefore, the control action is evaluated from an excited single-degree of freedom oscillator, represented by a three-dimensional system. Under this assumption, the control action changes the

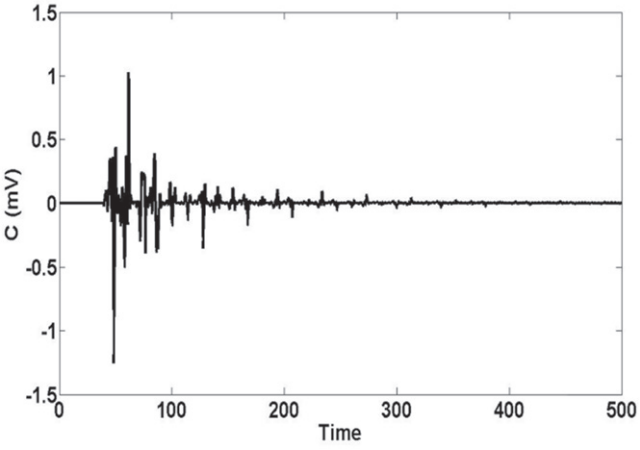

Figure 21. Control action for the stabilization of period-4 UPO.

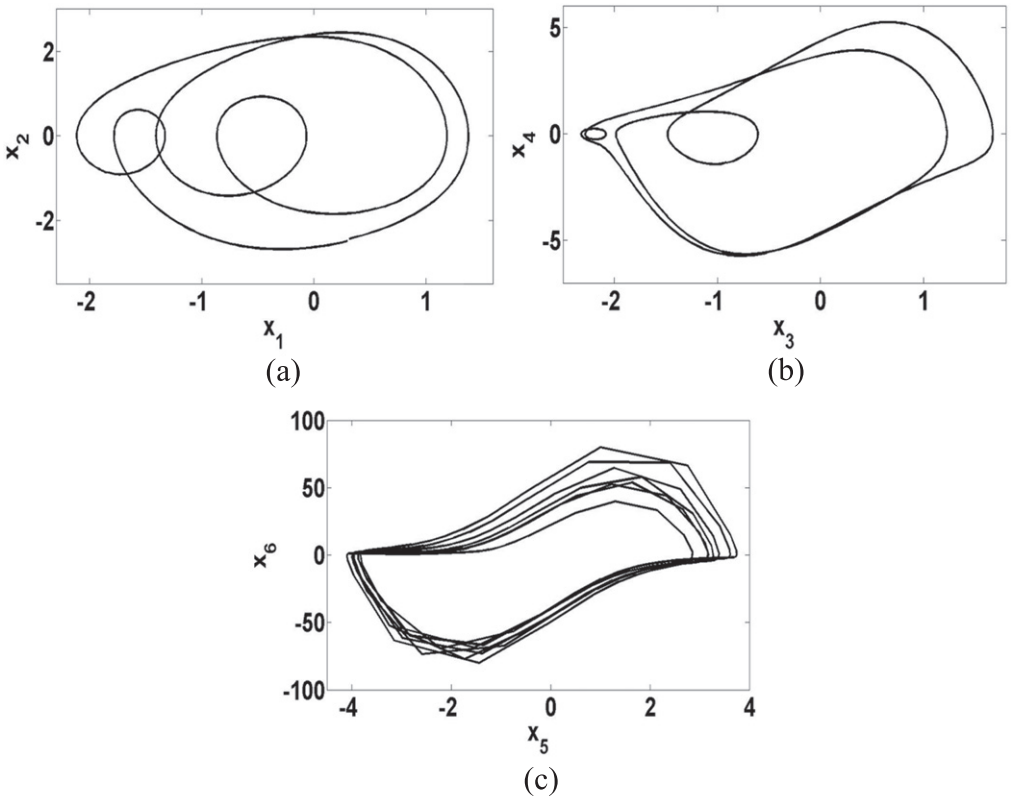

Figure 22. Identified period-4 UPO: (a) SA node, (b) AV node and (c) HP system.

system behavior by changing the SA node behavior. The coupled approach, on the other hand, treats the system as a seven-dimensional system related to three oscillators.

The uncoupled analysis of chaos control of the cardiac system is based on the natural pacemaker dynamics (SA node). Ferreira *et al* (2011) discussed the chaos control of this natural pacemaker, showing several situations related to that. The idea is to use the controlled signal of the natural pacemaker (SA node) as an input signal to the other systems (AV-HP subsystem). Hence, the control approach is split into two steps. The first one analyzes the SA node dynamics, governed by the following equation:

$$\begin{aligned}\dot{x}_1 &= x_2\\ \dot{x}_2 &= F(t) - \alpha(x_1 - v_1)(x_1 - v_2)x_2\\ &\quad -\frac{x_1(x_1 + d)(x_1 + e)}{ed} + C(t, x_2)\end{aligned} \tag{8}$$

The controlled signal is then applied to the other subsystem (AV-HP subsystem), governed by the following set of equations:

$$\begin{aligned}\dot{x}_3 &= x_4\\ \dot{x}_4 &= F_{AV}(t) - \alpha_{AV}x_4(x_3 - v_{AV_1})(x_3 - v_{AV_2})\\ &\quad -\frac{x_3(x_3 + d_{AV})(x_3 + e_{AV})}{d_{AV}e_{AV}}\\ &\quad -k_{SA-AV}\left(x_3 - x_1^{\tau_{SA-AV}}\right) - k_{HP-AV}\left(x_3 - x_5^{\tau_{HP-AV}}\right)\end{aligned}$$

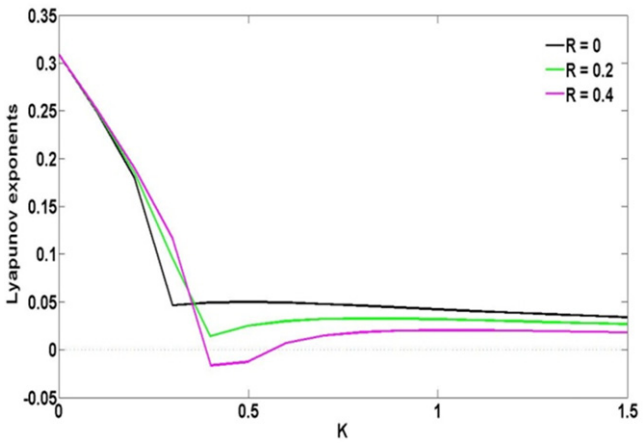

Figure 23. Period-4 UPO: maximum Lyapunov exponents.

$$\begin{aligned}\dot{x}_5 &= x_6\\ \dot{x}_6 &= F_{HP}(t) - \alpha_{HP}x_6(x_5 - v_{HP_1})(x_5 - v_{HP_2})\\ &\quad -\frac{x_5(x_5 + d_{HP})(x_5 + e_{HP})}{d_{HP}e_{HP}}\\ &\quad -k_{SA-HP}\left(x_5 - x_1^{\tau_{SA-HP}}\right) - k_{AV-HP}\left(x_5 - x_3^{\tau_{AV-HP}}\right)\end{aligned} \tag{9}$$

Under this assumption, the controller decouples both subsystems and all control details are evaluated just from

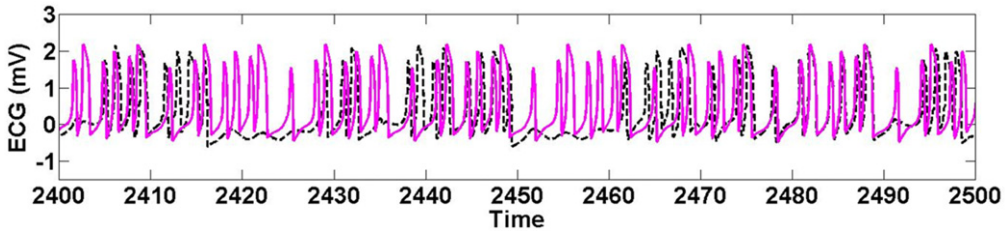

Figure 24. ECG related to ventricular fibrillation and the stabilization of a period-4 UPO: uncontrolled (dashed black line) and controlled (solid pink line) responses using $R = 0.4$ and $K = 0.4$.

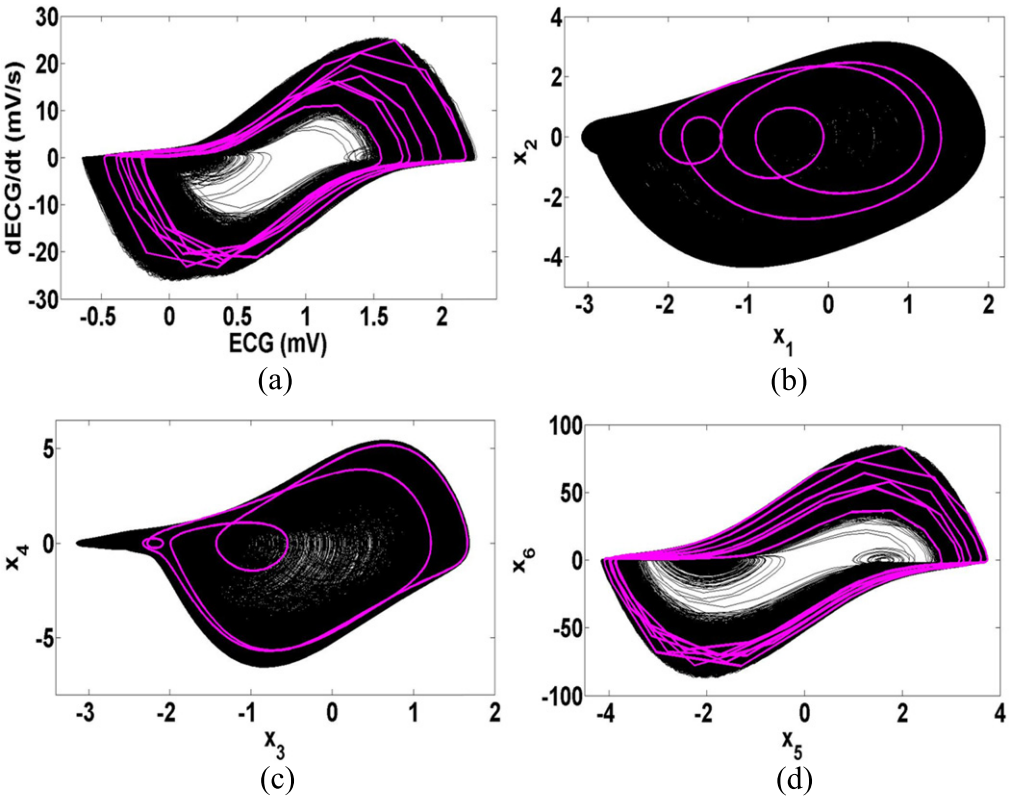

Figure 25. Phase space projections related to chaotic ECG and the stabilization of a period-4 UPO: uncontrolled (black line) and controlled (pink line) responses using $R = 0.4$ and $K = 0.4$. (a) ECG, (b) SA node, (c) AV node and (d) HP system.

the SA node. Therefore, the learning stage is related to only one oscillator and either UPOs' identification or controller parameters, K and R, are calculated from this single-degree of freedom oscillator. This uncoupled approach allows the use of a simpler system to evaluate controller parameters using a single-degree of freedom system, being easier than the coupled one, and obtaining the same results.

Nevertheless, it is important to highlight that some UPOs are only found in the whole system, represented by the coupled approach. Except for the second period-4 UPO discussed in the previous section (figures 22–26) that is identified only by the coupled approach, all other UPOs are identified from both approaches. Moreover, it is important to highlight that this uncoupled approach does not cover all possible

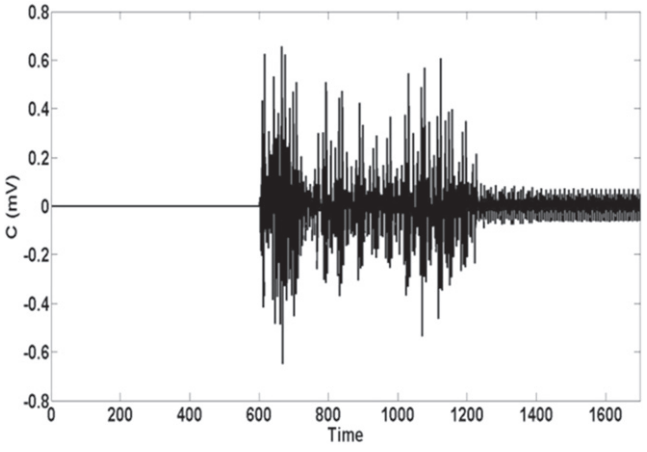

Figure 26. Control action for the stabilization of a period-4 UPO.

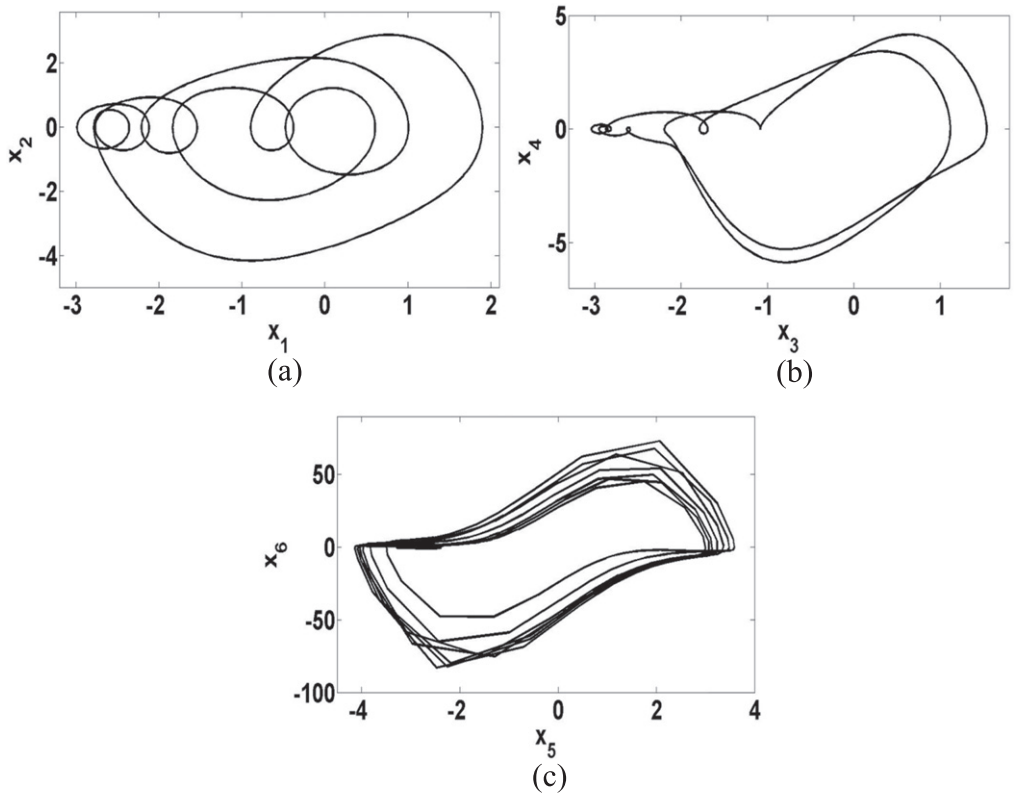

Figure 27. Identified period-7 UPO: (a) SA node, (b) AV node and (c) HP system.

pathological behaviors related to different couplings of the heart system.

5. Conclusions

This work deals with the application of the extended time-delayed feedback chaos control method to the cardiac system modeled as a three-coupled oscillator, connected with time delay couplings. Cardiac behavior is analyzed by considering ECG signals and two different situations are treated: normal and chaotic signals. Chaotic behavior of the heart can be understood as a critical pathological behavior and the basic idea is to employ ETDF method to avoid this critical behavior. We stabilize some UPOs embedded in the chaotic attractor, analyzing the resulting ECG. In general, it is possible to say that the ETDF is successfully applied generating less critical behaviors of the heart with small control efforts. Nevertheless, it is not an easy task to find the appropriate UPO related to the normal ECG, and therefore, this less critical behavior is not necessarily related to a normal ECG. An alternative approach is also investigated in order to suppress chaos with higher control efforts, by stabilizing orbits that do not belong to system dynamics. Finally, an uncoupled approach is discussed by considering a subsystem dynamics related to the SA node, mathematically represented by only one oscillator. The idea is to perform control on the natural pacemaker using the controlled signal as input signal for the other systems. This approach is associated with a three-dimensional system and therefore, has less computational effort. In general, it has been successfully applied to the chaotic response however, there are some pathologies that are not possible to be analyzed by this way. Besides, some dynamics characteristics are not observed in the reduced system, as some UPOs embedded in chaotic attractors. The application of chaos control method proves to be an interesting approach to avoid

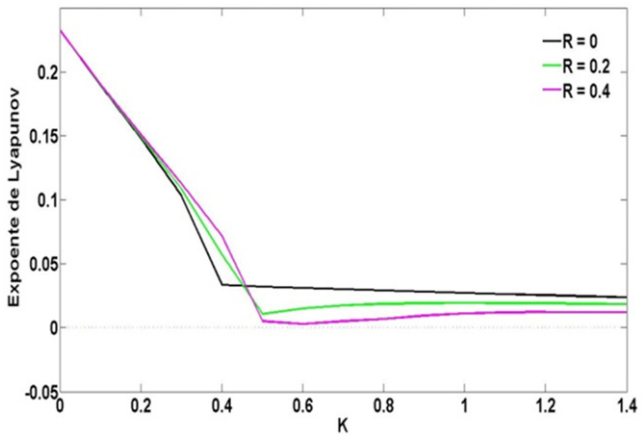

Figure 28. Period-7 UPO: maximum Lyapunov exponents.

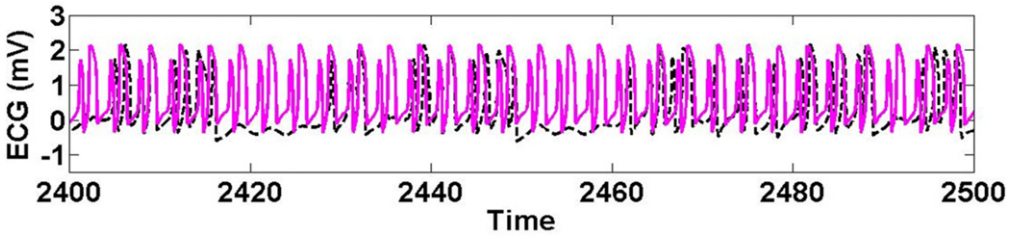

Figure 29. Chaotic ECG related and the chaos suppression: uncontrolled (dashed black line) and controlled (solid pink line) responses using $R = 0.8$ and $K = 2$.

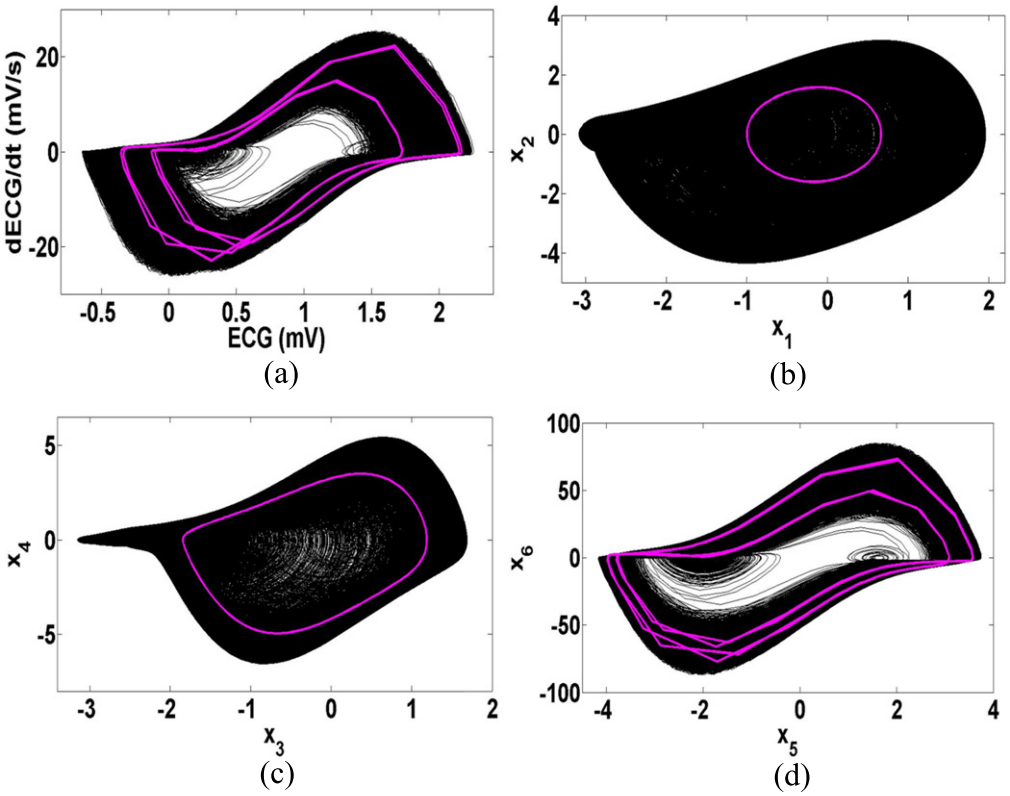

Figure 30. Phase space projections related to chaotic ECG and the chaos suppression: uncontrolled (black line) and controlled (pink line) responses using $R = 0.8$ and $K = 2$. (a) ECG, (b) SA node, (c) AV node and (d) HP system.

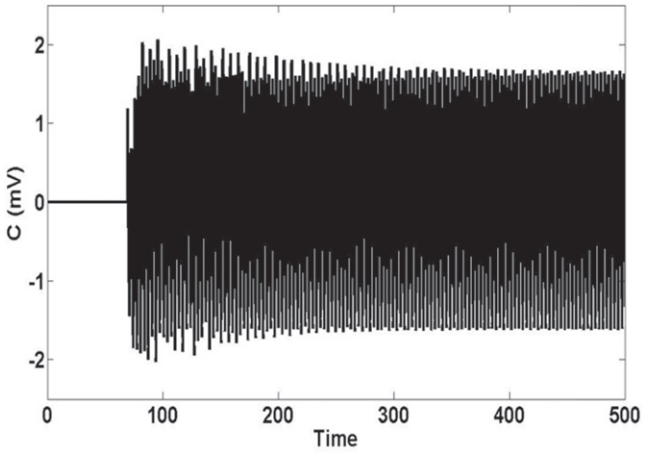

Figure 31. Control action for the chaos suppression using $R = 0.8$ and $K = 2$.

critical behaviors related to chaotic behavior with small control efforts. Situations where chaos control does not succeed can be easily solved by increasing the control effort, which leads to the suppression of chaotic response. The authors believe that the presented results encourage the idea that this approach can be employed in pacemakers. Nevertheless, experimental tests are important to confirm this conclusion defining the best way for its application.

Acknowledgements

The authors would like to acknowledge the support of the Brazilian Research Agencies CNPq, CAPES and FAPERJ and through the INCT-EIE (National Institute of Science and Technology—Smart Structures in Engineering) the CNPq and

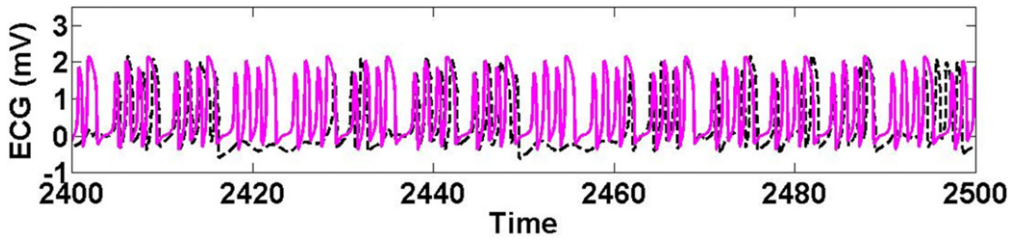

Figure 32. Chaotic ECG and the chaos suppression: uncontrolled (dashed black line) and controlled (solid pink line) responses using $R = 0.9$ and $K = 0.6$.

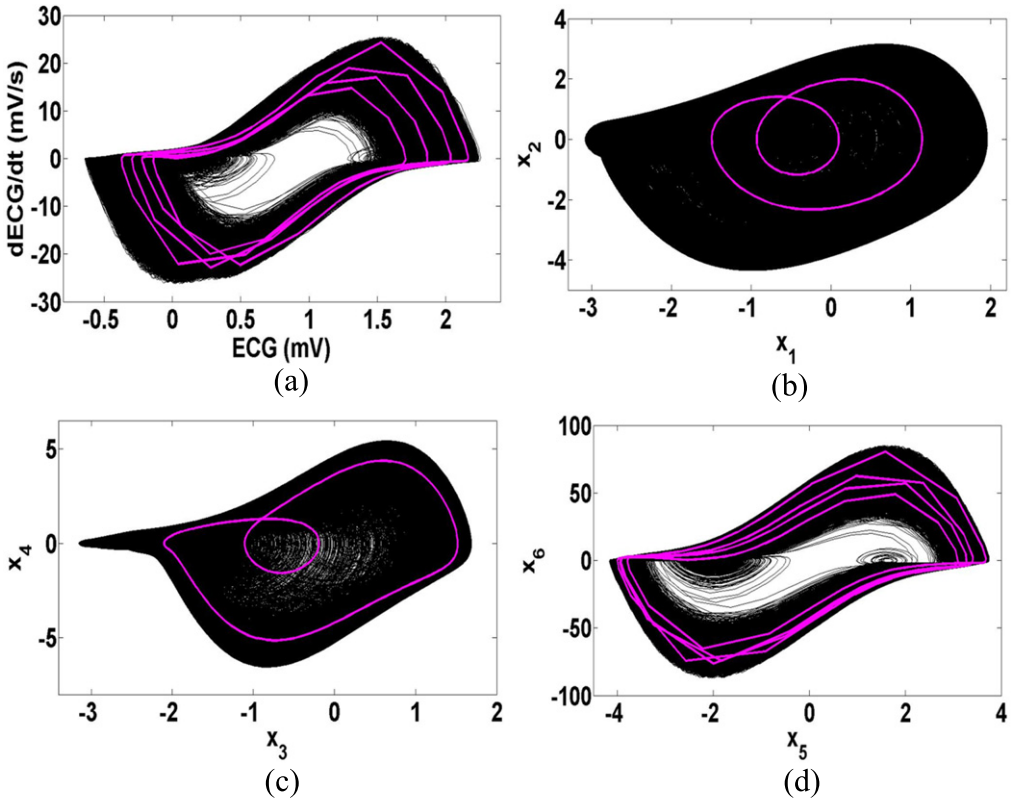

Figure 33. Phase space projections related to chaotic ECG and the chaos suppression: uncontrolled (black line) and controlled (pink line) responses using $R = 0.9$ and $K = 0.6$. (a) ECG, (b) SA node, (c) AV node and (d) HP system.

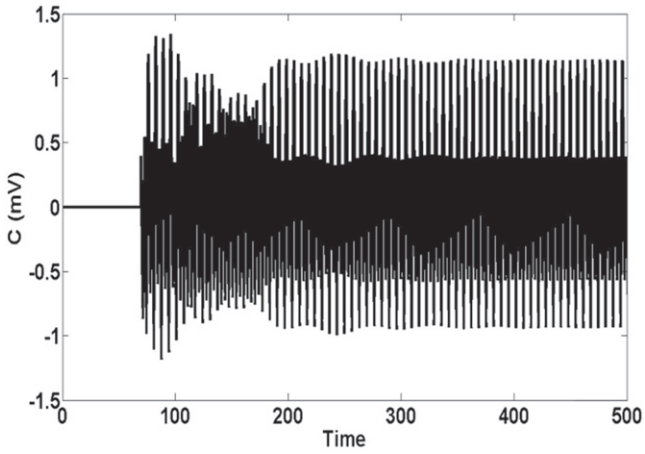

Figure 34. Control action for the chaos suppression.

FAPEMIG. The Air Force Office of Scientific Research (AFOSR) is also acknowledged.

References

Andrievskii B R and Fradkov A L 2004 Control of chaos: methods and applications. II. Applications *Automation and Remote Control* **65** 505–33

Attarsharghi S, Jahed-Motlagh M R, Vasegh N and Khaki-Sedigh A 2009 Adaptive control of chaos in cardiac arrhythmia *Mechanical and Electronics Engineering* 49–53

Auerbach D, Predrag C, Eckmann J P, Gunaratne G and Procaccia I 1987 Exploring chaotic motion through periodic orbits *Phys. Rev. Lett.* **58** 2387–9

Boccaletti S, Grebogi C, Lai Y–C, Mancini H and Maza D 2000 The control of chaos: theory and applications *Phys. Rep.* **329** 103–97

Christini D J, Stein K M, Markowitz S M, Mittal S, Slotwiner D J, Scheiner M A, Iwai S and Lerman B B 2001 Nonlinear-dynamical arrhythmia control in humans *Medical Sciences* **98** 5827–32

Cunningham W J 1954 A nonlinear differential-difference equation of growth *Mathematics* **40** 708–13

De Paula A S and Savi M A 2008 A multiparameter chaos control method applied to maps *Braz. J. Phys.* **38** 537–43

De Paula A S and Savi M A 2009a Controlling chaos in a nonlinear pendulum using an extended time-delayed feedback method *Chaos Solitons Fractals* **42** 2981–8

De Paula A S and Savi M A 2009b A multiparameter chaos control method based on OGY approach *Chaos Solitons Fractals* **40** 1376–90

De Paula A S and Savi M A 2011 Comparative analysis of chaos control methods: a mechanical system case study *Int. J. Non-Linear Mech.* **46** 1076–89

De Paula A S, Savi M A, Wiercigroch M and Pavlovskaia E 2012 Bifurcation control of a parametric pendulum *Int. J. Bifurcation Chaos Appl. Sci. Eng.* **22** 1–14 Article 1250111

Dubin D 1996 *Interpretação Rápida do ECG: Um Curso Programado* (Rio de Janeiro: Publicações Científicas)

Dubljevic S, Lin S F and Christofides P D 2008 Studies on feedback control of cardiac alternans *Comput. Chem. Eng.* **32** 2086–98

Farmer J D 1982 Chaotic attractors of an infinite-dimensional dynamical system *Physica 4D* **55** 366–93

Ferreira B B, De Paula A S and Savi M A 2011 Chaos control applied to heart rhythm dynamics *Chaos Solitons Fractals* **44** 587–99

Fradkov A L, Evans R J and Andrievsky B R 2006 Control of chaos: methods and applications in mechanics *Phil. Trans. R. Soc.* A **364** 2279–307

Garfinkel A, Spano M L, Ditto W L and Weiss J N 1992 Controlling cardiac chaos *Science* **257** 1230–5

Garfinkel A, Weiss J N, Ditto W L and Spano M L 1995 Chaos control of cardiac arrhythmias *Trends in Cardiovascular Medicine* **5** 76–80

Glass L, Guevara M R, Shrier A and Perez R 1983 Bifurcation and chaos in a periodically stimulated cardiac oscillator *Physica 7D* 89–101

Glass L, Goldberger A L, Courtemanche M and Shrier A 1987 Nonlinear dynamics, chaos and complex cardiac arrhythmias *Proc. R. Soc. Lond.* **413** 9–26

Gois S R S M and Savi M A 2009 An analysis of heart rhythm dynamics using a three-coupled oscillator model *Chaos Solitons Fractals* **41** 2553–65

Grudzinski K and Zebrowski J J 2004 Modeling cardiac pacemakers with relaxation oscillators *Physica* A **336** 153–62

Hall K, Christini D J, Tremblay M, Collins J J, Glass L and Billette J 1997 Dynamic control of cardiac alternans *Phys. Rev. Lett.* **78** 4518–21

Hubinger B, Doerner R, Martienssen W, Herdering M, Pitka R and Dressler U 1994 Controlling chaos experimentally in systems exhibiting large effective lyapunov exponents *Phys. Rev.* E **50** 932–48

Kapitaniak T 1995 Continuous control and synchronization in chaotic systems *Chaos Solitons Fractals* **6** 237–44

Kaplan D T and Cohen R J 1990 Is fibrillation chaos? *Circ. Res.* **67** 886–92

Korte R J D, Schouten J C and Bleek C M van den 1995 Experimental control of a chaotic pendulum with unknown dynamics using delay coordinates *Phys. Rev.* E **52** 3358–65

López M J, Consegliere A, Lorenzo J and García L 2010 Computer simulation and method for heart rhythm control based on ECG signal reference tracking *WSEAS Transactions on Systems* **9** 263–72

Mensour B and Longtin A 1997 Power spectra and dynamical invariants for delay-differential and difference equations *Physica* D **113** 1–25

Muthukumar P and Balasubramaniam P 2013 Feedback synchronization of the fractional order reverse butterfly-shaped chaotic system and its application to digital cryptography *Nonlinear Dyn.* **74** 1169–81

Muthukumar P, Balasubramaniam P and Ratnavelu K 2014 Synchronization of a novel fractional order stretch-twist-fold (STF) Flow chaotic system and its application to a new authenticated encryption scheme (AES) *Nonlinear Dyn.* doi:10.1007/s11071-014-1398-x.

Ott E, Grebogi C and Yorke J A 1990 Controlling chaos *Phys. Rev. Lett.* **64** 1196–9

Pyragas K 1992 Continuous control of chaos by self-controlling feedback *Phys. Lett.* A **170** 421–8

Pyragas K 1995 Control of chaos via extended delay feedback *Phys. Lett.* A **206** 323–30

Pyragas K 2006 Delayed feedback control of chaos *Phil. Trans. R. Soc.* A **364** 2309–34

Santos A M, Lopes S R and Viana R L 2004 Rhythm synchronization and chaotic modulation of coupled Van der Pol oscillators in a model for the heartbeat *Physica* A **338** 335–55

Savi M A 2005 Chaos and order in biomedical rhythms *Journal of the Brazilian Society of Mechanical Sciences and Engineering* **27** 157–69

Shinbrot T, Grebogi C, Ott E and Yorke J A 1993 Using small perturbations to control chaos *Nature* **363** 411–7

Socolar J E S, Sukow D W and Gauthier D J 1994 Stabilizing unstable periodic orbits in fast dynamical systems *Phys. Rev.* E **50** 3245–8

Stein K M, Walden J, Lippman N and Lerman B B 1999 Ventricular response in atrial fibrillation: random or deterministic? *American Journal of Physiology—Heart and Circulatory Physiology* **277** H452–8

Van der Pol B and Van der Mark J 1928 The heartbeat considered as a relaxation oscillator and an electrical model of the heart *Phil. Mag.* **6** 763–75

Witkowski F X, Kavanagh K M, Penkoske P A, Plonsey R, Spano M L, Ditto W L and Kaplan D T 1995 Evidence for determinism in ventricular fibrillation *Phys. Rev. Lett.* **75** 1230–3

Witkowski F X, Leon L J, Penkoske P A, Giles W R, Spano M L, Ditto W L and Winfree A T 1998 Spatiotemporal evolution of ventricular fibrillation *Nature* **392** 78–82

Wolf A, Swift J B, Swinney H L and Vastano J A 1985 Determining lyapunov exponents from a time series *Physical* D **16** 285–317